INSTITUTE OF PHYSICS PUBLISHING NANOTECHNOLOGY
Nanotechnology **14** (2003) L11–L14 PII: S0957-4484(03)64582-4

LETTER TO THE EDITOR

Adhesion study of polyimide to single-wall carbon nanotube bundles by energy-filtered transmission electron microscopy

Cheol Park[1,5], Roy E Crooks[2], Emilie J Siochi[3], Joycelyn S Harrison[3], Neal Evans[4] and Edward Kenik[4]

[1] National Institute of Aerospace, 144 Research Drive, Hampton, VA 23666, USA
[2] Swales, NASA Langley Research Center, MS-188A, Hampton, VA 23681-2199, USA
[3] Advanced Materials and Processing Branch, NASA Langley Research Center, MS-226, Hampton, VA 23681-2199, USA
[4] Metals and Ceramics Division, Oak Ridge National Lab, PO Box 2008, Oak Ridge, TN 37831, USA

E-mail: c.park@larc.nasa.gov

Received 4 June 2003
Published 11 August 2003
Online at stacks.iop.org/Nano/14/L11

Abstract
High-resolution electron microscopy and energy-filtered imaging methods were used to examine single-wall carbon nanotubes and nanotube reinforced polyimide composites. The nanotubes were studied alone, in a polyimide matrix composite, and after deposition of composite material previously dissolved in a solvent. Energy-filtered images based on nitrogen core loss excitations were used to discern the presence of polyimide. Elemental maps of nanotubes extracted from the composite revealed good wetting of the nanotube surfaces by the polyimide.

(Some figures in this article are in colour only in the electronic version)

1. Introduction

Carbon nanotubes (CNT) have been extensively studied since their discovery by Iijima in 1991 [1]. In particular, single-wall carbon nanotubes (SWNT) have attracted a great deal of attention because of superior combinations of electrical, mechanical and thermal properties. Taking advantage of these superior properties on a macroscopic scale is facilitated by incorporation of the SWNT into a polymer matrix composite. High temperature polymers, e.g. polyimides, have been developed for aerospace and electronics applications and significant benefits in strength and electrical properties are expected from SWNT reinforcement. Although numerous studies have described SWNT–polymer matrix composites, uniform dispersion of SWNT in a polymer matrix is difficult due to a lack of adhesion between the polymer and SWNT [2–4]. There are also difficulties involved in characterization. Uniform dispersion and effective reinforcement by SWNT in a polymer matrix requires wetting of the non-reactive SWNT surface by the solvated polymer during production. In this study a polyimide, an aromatic polar polymer, was selected for chemical compatibility with the SWNT surface. Interfacial adhesion in this aromatic polymer/SWNT nanocomposite is promoted by favourable overlap interactions between the polymer and the SWNT [5, 6] and a donor–acceptor interaction via charge transfer [7]. These interactions result in better adhesion than that possible with van der Waals interactions alone. Previous work has shown that the addition of 0.1 wt% SWNT to a polyimide matrix results in an electrical

[5] Author to whom any correspondence should be addressed.

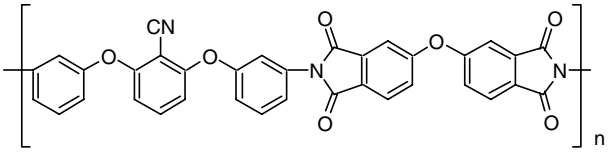

Figure 1. Chemical structure of (β-CN)APB/ODPA.

conductivity increase of 10 orders of magnitude without a significant loss in optical transmission. Both mechanical properties and thermal stability were also improved [8]. This superb reinforcing efficiency presumably arises from adhesion of the polyimide to the SWNT surface, which leads to effective dispersion of the SWNT. This study reports evidence of adhesion of a polymer to SWNT surfaces within an effectively reinforced composite.

2. Experimental details

A batch of purified laser ablated SWNT was obtained from Rice University. TEM and AFM observations revealed a SWNT diameter of approximately 1.4 nm and a length of individual tubes of approximately 3 μm [9]. An aromatic polyimide, (β-CN)APB/ODPA [10], was selected as a polymer matrix and the chemical structure is shown in figure 1. The (β-CN)APB/ODPA was prepared from 2,6-*bis*(3-aminophenoxy) benzonitrile ((β-CN)APB) and 4,4′ oxidiphthalic anhydride (ODPA) in *N*, *N*-dimethylacetamide (DMAc) via a poly(amic acid) solution. The details of the synthesis were described elsewhere [11].

A dilute SWNT solution, typically around 0.05 wt% in DMAc, was prepared by homogenizing for 10 min (750 rpm with a 6 mm diameter rotor homogenizer) and sonicating for an hour at 47 kHz. The sonicated SWNT solution was used as a solvent for the poly(amic acid) synthesis with the diamine and dianhydride. The entire reaction was carried out with stirring in a nitrogen-purged flask immersed in a 40 kHz ultrasonic bath until the solution viscosity increased and stabilized. Sonication was ceased and stirring was continued for several hours to form a SWNT–poly(amic acid) solution.

SWNT–polyimide nanocomposite films were prepared with a SWNT concentration of 0.5 wt%. The SWNT–poly(amic acid) solution prepared was cast onto a glass plate and dried in a dry air-flowing chamber. Subsequently, the dried tack-free film was thermally imidized in a nitrogen-circulating oven to obtain a solvent-free free-standing SWNT–polyimide film. For the TEM study, film specimens were re-dissolved in the aprotic solvent used for the synthesis and sonicated for three hours at 47 kHz. The re-dispersed dilute solution was deposited on a holey carbon film on a copper grid. SWNT bundles and re-dissolved films were examined in a Philips CM200 TEM, with a LaB6 filament operated at 200 kV, and a similar instrument with a field emission source. Energy-filtered images of solute-isolated nanotube bundles were collected with a Gatan GIF system on a Philips CM30, with a LaB6 filament operated at 200 kV. Elemental maps were obtained using a standard three-window technique that assumed an Ae^{-r} model for the background. For elemental maps the window included the K-absorption edge, and background subtractions were based on curve fitting from two pre-edge maps and one post-edge map for each element.

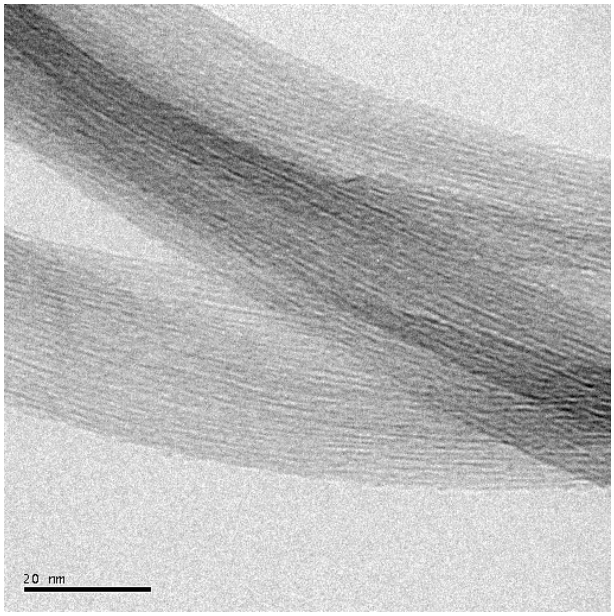

Figure 2. Energy-filtered, 200 keV, zero-loss HREM image of bundles of purified, laser ablated SWNT over a hole in a holey carbon film.

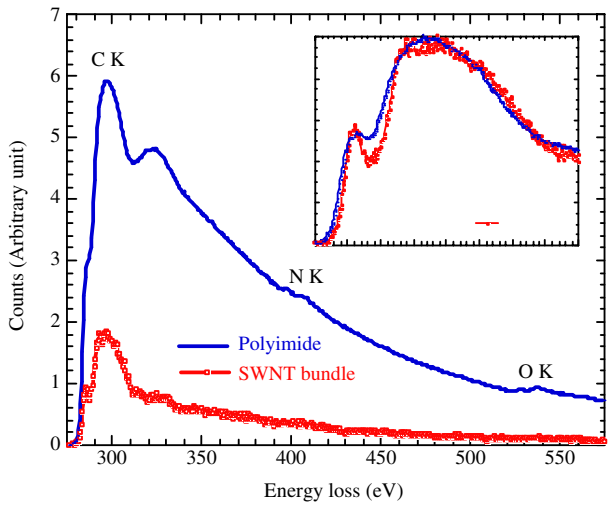

Figure 3. Electron energy loss spectra of the pure SWNT and the polyimide. Carbon K (1s) absorption edges of the SWNT and the polyimide are shown in the inset.

3. Results and discussion

Figure 2 shows a TEM micrograph of as-received purified SWNT bundles. The nanotube contrast appears most strongly at defocus of 100–200 nm. Focus was determined at the edge of a nanotube bundle and defocused until the maximum nanotube contrast was observed. The image was collected at a defocus of 150 nm, with imaging conditions set to minimize beam damage and thermal drift in the area of interest. Cross-sectional dimensions were not determined, but focusing experiments indicate that they are closer to rounded bundles than to flat ribbons. Two bundles are shown with diameters near 40 nm. Single-carbon nanotube diameters are approximately 1.4 nm.

Electron energy loss spectra of the pure SWNT and the polyimide are shown in figure 3. A typical carbon K (1s) absorption edge of the SWNT is shown in the inset of figure 3,

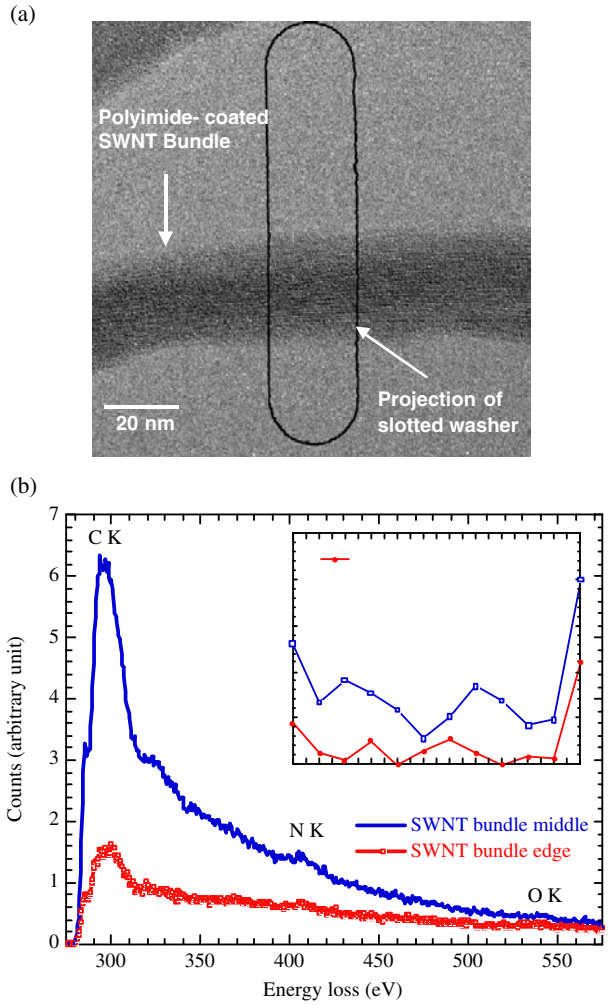

Figure 4. (a) Zero-loss TEM image of a polyimide-coated SWNT bundle and the area selected for EELS. (b) EELS spectra of the selected area. The N/C ratio from one edge of the polyimide-coated SWNT bundle to the other edge is shown in the inset.

where a sharp π^* and broad σ^* appeared at 285 and 292 eV, respectively. The relatively low ratio of π^* to σ^* is attributed to the small curvature of the tube surface. The π^* in polyimide in the inset was not so well defined as that of SWNT. The (β-CN)APB/ODPA polyimide $(C_{35}N_3O_7H_{17})_n$ used in this study contains three nitrogen atoms in the monomer, as shown in figure 1. Nitrogen can provide a contrast in the EELS spectra between the polyimide-coated SWNT bundle and the bare SWNT bundles, as shown in figure 3. The nitrogen peak allows energy-filtered imaging to distinguish the polyimide from the SWNT when a sufficiently strong signal is obtained. Spatially resolved EELS spectral lines were acquired across bundles to determine nitrogen/carbon atomic ratios across the bundle. Figure 4(a) shows a zero-loss TEM image of a polyimide-coated SWNT bundle and the area selected for EELS. Area selection was controlled by use of a slotted washer (2×0.5 mm au) located in the GIF entrance aperture and oriented normal to the energy dispersion direction. The EELS spectra were obtained from one edge of the polyimide-coated SWNT bundle to the other edge. Polyimide on the SWNT bundle was identified from the nitrogen signal in the EELS spectra acquired from the middle and edges of the coated bundle in figure 4(b). The inset of figure 4(b) shows the N/C ratio across the polyimide-coated SWNT bundle, indicating that the ratio increases when approaching the near edges and lowest near middle of the bundle. This N/C ratio profile reasonably suggests that the whole of the SWNT bundles were uniformly coated with the polyimide.

Figure 5(a) shows a zero energy loss image of the redissolved SWNT–polyimide nanocomposite on a holey carbon film. Polyimide-coated SWNT bundles are seen across the holes and on the amorphous carbon substrate with rounded polymer beads. The curved white band on the left side of figure 5(a) is due to a camera defect. Polymer beads had different sizes and often appeared to encompass and wick the SWNT bundles. Energy-filtered transmission electron microscopy (EFTEM) elemental maps were obtained from this area, and a nitrogen elemental map is shown in figure 5(b). EFTEM mapping was problematic due to beam interactions with the SWNT bundles. Relative image drift correction across the entire image (figure 5(b)) is imperfect due to slight translations and rotations of those bundles lying across the holes. The direction of bright–dark contrast reversals along the edges of the features, which is indicative of relative drift, is not constant across the image. On the other hand, bundles on the carbon substrate did not drift as much as those on the holes, possibly due to the substrate acting as a local heat sink or by adding structural stability to the bundles. For figure 5(b), component images were aligned to minimize the relative drift in the small bundle. The irregular cross section of the SWNT bundles in figure 5 can be attributed to either

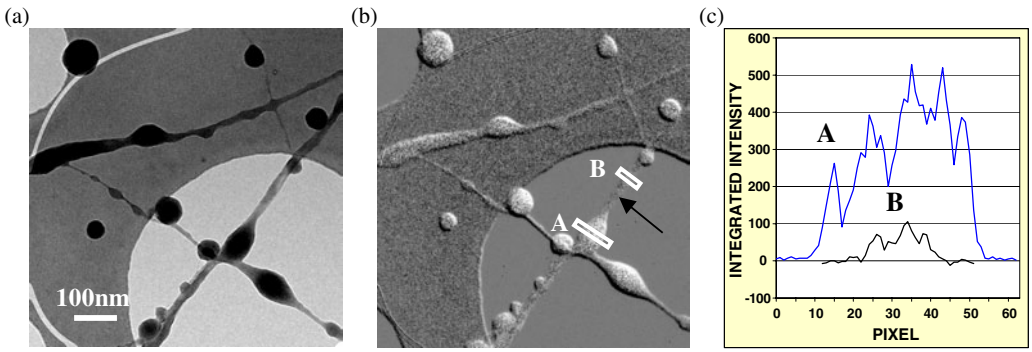

Figure 5. (a) Zero energy loss image of the redissolved SWNT–polyimide nanocomposite on a holey carbon film. (b) EFTEM nitrogen elemental map were obtained from the area (a). (c) Integrated intensity profiles acquired from regions marked A and B in (b).

adherent polyimide or to features associated with the bundles. The nitrogen elemental map in figure 5(b) shows these features to be due to coating by the polymer. Even a 2 nm thick SWNT feature (upper right in figure 5(b)) shows high nitrogen content relative to the background, indicating that the tube was uniformly coated with the polyimide. The integrated intensity profiles in figure 5(c), acquired from the regions marked A and B in the nitrogen elemental map, may reliably be used to indicate the nitrogen contained in the polyimide. A similar oxygen elemental map for the same area was obtained as well. The low contact angle of polymer droplets in contact with the SWNT bundles also indicates good wetting, while the polymer only in contact with the amorphous carbon tended to form rounded beads due to the lower surface energy of the amorphous carbon. This is evident from the spherical droplets on the carbon support film seen on the left side of figures 5(a). Similar methods, using TEM in combination with contact angle experiments, may be used to evaluate surface treatments to improve wetting of SWNT.

In summary, aromatic polar polymers, such as polyimide, show promise as matrix materials for CNT composites. Examination of SWNT bundles extracted from (β-CN) polyimide matrix composites shows wetting of bundle surfaces by the polyimide. This is confirmed by electron energy loss nitrogen elemental mapping, which revealed the distribution of the (β-CN) polyimide on SWNT bundles.

Acknowledgments

Research at the Oak Ridge National Laboratory SHaRE Collaborative Research Center was sponsored by the Division of Materials Sciences and Engineering, US Department of Energy, under contract DE-AC05-00OR22725 with UT-Battelle, LLC. The authors are grateful for suggestions from Dr J Bentley at ORNL and for the support of Dr J S Harrison at NASA Langley.

References

[1] Iijima S 1991 *Nature* **354** 56
[2] Chen J, Hamon M A, Hu H, Chen Y, Rao A M, Eklund P C and Haddon R C 1998 *Science* **282** 95
[3] Mickelson E T, Huffman C B, Rinzler A G, Smalley R E, Hauge R H and Margrave J L 1998 *Chem. Phys. Lett.* **296** 188
[4] Bahr J L and Tour J 2001 *Chem. Mater.* **13** 3823
[5] Curran S, Ajayan P M, Blau W, Carroll D L, Coleman J N, Dalton A B, Davey A P, Drury A, McCarthy B, Maier S and Strevens A 1998 *Adv. Mater.* **10** 1091
[6] Chen R J, Zhang Y, Wang D and Dai H 2001 *J. Am. Chem. Soc.* **123** 3838
[7] Wise K E, Park C and Siochi E J 2003 *Chem. Phys. Lett.* submitted
[8] Park C, Ounaies Z, Watson K A, Crooks R E, Lowther S E, Connell J W, Siochi E J, Harrison J S and St Clair T L 2002 *Chem. Phys. Lett.* **364** 303
[9] Lillehei P T, Rouse J, Park C and Siochi E J 2002 *Nano. Lett.* **2** 827
[10] Simpson J O, Welch S S and St Clair T L 1996 *Proc. Materials Research Society Symp.: Materials for Smart Systems II* vol 413 (Warrendale, PA: Materials Research Society) p 351
[11] Simpson J O, Ounaies Z and Fay C 1997 *Proc. Materials Research Society Symp.: Materials for Smart Systems II* vol 459 (Warrendale, PA: Materials Research Society) p 59